Journal of Applied and Computational Mechanics, Vol. 2, No. 2, (2016), 96-117

Shahid Chamran University

Journal of
Applied and Computational Mechanics

Concerning the Effect of a Viscoelastic Foundation on the Dynamic Stability of a Pipeline System Conveying an Incompressible Fluid

Vincent O. S. Olunloyo[1], Charles A. Osheku[2], Patrick S. Olayiwola[3]

[1] Department of Systems Engineering, Faculty of Engineering, University of Lagos, Akoka-Yaba, Lagos 23401, Nigeria.vosolunloyo@hotmail.com

[2] Centre for Space Transport and Propulsion, National Space Research and Development Agency Federal Ministry of Science and Technology, FCT, PMB 437, Abuja, Nigeria.charlesosheku2002@yahoo.com

*On leave of absence from the Department of Systems Engineering, Faculty of Engineering, University of Lagos.

[3] Department of Mechanical & Biomedical Engineering, College of Engineering, Bells University of Technology, Ota, Ogun State 234037, Nigeria. olayiwola_patrickshola@yahoo.com

Received July 14 2016; revised October 12 2016; accepted for publication November 11 2016.
Corresponding author: Patrick S. Olayiwola, olayiwola_patrickshola@yahoo.com

Abstract

In this paper, we present an analytical method for solving a well-posed boundary value problem of mathematical physics governing the vibration characteristics of an internal flow propelled fluid-structure interaction where the pipeline segment is idealized as an elastic hollow beam conveying an incompressible fluid on a viscoelastic foundation. The effect of Coriolis and damping forces on the overall dynamic response of the system is investigated. In actuality, for a pipe segment supported at both ends and subject to a free motion, these two forces generate conjugate complex frequencies for all flow velocities. On employing integral transforms and complex variable functions, a closed form analytical expression is derived for the overall dynamic response. It is demonstrated that a concise mathematical expression for the natural frequency associated with any mode of vibration can be deduced from the algebraic product of the complex frequency pairs. By a way of comparative analysis for damping decrement physics reminiscent with laminated structures, mathematical expressions are derived to illustrate viscoelastic damping effects on dynamic stability for any flow velocity. The integrity of the analytical solution is verified and validated by confirming theresults in literature in appropriate asymptotic limits.

Keywords: Analytical method, viscoelastic foundation, Coriolis and damping forces, conjugate complex frequency pairs and damping decrement physics.

1. Introduction

Engineering examples of fluid-conveying slender systems interacting with axial flow abound in practice. Other examples include flexible conduits containing flowing fluid, heat-exchanger tubes in axial flow regions of the secondary fluid and containing internal flow of the primary fluid, nuclear reactor fuel elements, monitoring and control tubes, thin-shell structures used as heat shields in aircraft engines and nuclear reactors. Nonetheless, further engineering devices include jet pumps, certain types of valves and other components in hydraulic machinery, towed slender ships, barges and submarine systems, etc. Physiological examples may be found in the pulmonary and urinary systems and in haemodynamics.

As rightly pointed out by Paidoussis [1], although the work on the dynamics of pipes conveying fluid has mostly been curiosity-driven over the years, it has nonetheless yielded rich rewards among which are : (i) the development of theory for certain classes of dynamical systems, and of new analytical methods for such systems; (ii) the understanding of the dynamics of more complex systems (such as the investigation of the dynamics and stability of fluid-conveying curved and twisted pipes in complex spatial forms), and (iii) the direct use of this work in some a priori unforeseen practical applications.

For the fluid-conveying pipelines, it is common to observe Coriolis force components among the terms describing the mathematical models of the system. This term has drawn researchers and engineering physicists into probing its significance within the system. Mostafa [2] investigated the natural frequency of a simply supported pipeline (hinged type) conveying 1-D incompressible steady fluid flow set on a viscoelastic foundation. He stated that the Coriolis acceleration term arises because the fluid flows with a velocity relative to the pipe, such that it causes the fluid-structural interaction model to belong to the class of complex eigenvalue problems. It is noted in [2] that during free oscillations the Coriolis force term does no work, i.e., it dissipates no energy. This term is also identified as a nonworking velocity-dependent load called gyroscopic by [3,6]. Confirmation of this is provided by the experimental work reported in [4, 5]. In the 1950s, proofs were claimed of researchers and mathematicians' works showing that the Coriolis has negligible effects even at the molecular scale level of interaction. However, as pointed out in [1], granted that the gyroscopic (Coriolis) forces do no work in the course of free motions, but they nonetheless can exert important influence on the overall dynamical behavior of a pipeline system.

It is observed that suppression of instability is a peculiar factor in some pipeline systems. A number of efforts have been made by researchers to examine effects of different foundation on such systems. Fluid-conveying pipes that rest on elastic foundations were examined by Lottati and Kornecki [7], where he found that the critical flow velocity of fluid-conveying pipe resting on a Winkler foundation is higher than that without a foundation. Others in a similar investigation are Stein and Tobriner [8], Dermendijan-Ivanova [9], Chary et al [10] and Doarre et al [11]. Recently, Chellapilla and Simha [12] studied the problem of vibration of fluid-conveying pipes on a two-parameter foundation model – the Pasternak-Winkler model, while Mahrenholtz [13] extended the Winkler's model to account for the effect of time dependence in the simplest case to make it viscous, so that he applied the viscous model to solve a problem of rotating wheel sets on polymer rubber sheets. In other methods, instabilities suppression were investigated via the use Eddy current dampers by Saxena and Patel [14], Jae-Sung et al [15] and Tonoli [16].

In the recent work by Olayiwola [17], a direct method was used to investigate a fluid-conveying pipeline system that is resting on a visco-elastic foundation via integral transforms. Szmidt and Przybylowicz [18] studied the influence of electromagnetic damping on the dynamics of a pipe conveying fluid and observed that within such a context, the Coriolis effect is seen to be a destabilizing one. Kuye [19] investigated the effects of piping material viscoelasticity and the deformable sea bed foundation on offshore fluid-conveying pipes.

This paper presents exact closed-form solutions for the natural frequencies, and demonstrates the dependence of the complex natural frequencies on the Coriolis and damping forces, and the rational natural frequency of the system. Also, the effects of Coriolis and damping forces on the dynamic response of the system are highlighted and presented.

2. Analysis of an Euler Beam Conveying an Incompressible fluid

An analysis of the bending of a beam on a viscoelastic foundation based on the Winkler model is derived from the assumption that the foundation's reaction forces are proportional at every point, to the deflection of the beam at that point. The differential equation of the elastic line is based on the notion that the straight beam is supported along its entire length by a viscoelastic medium and subjected to vertical forces in the principal plane of the symmetrical cross section (see Figure 1).

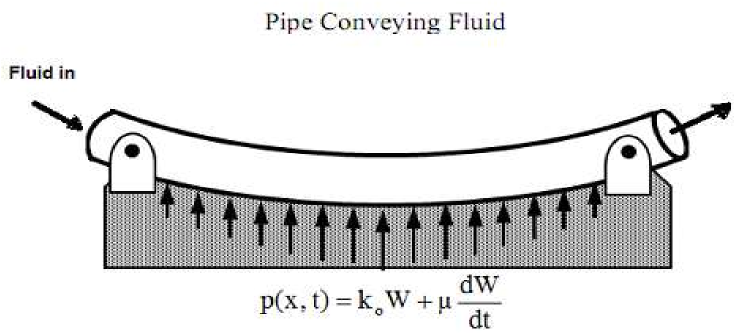

Fig. 1. Representation of modified Winkler foundation model

The partial differential equation governing the dynamics of a fluid-conveying pipeline segment supported on a viscoelastic foundation (Mostafa [2]) is

$$EI\frac{\partial^4 w}{\partial x^4}+k_0 w+\rho_f U^2\frac{\partial^2 w}{\partial x^2}+\left(\rho_p+\rho_f\right)\frac{\partial^2 w}{\partial t^2}+\mu\frac{\partial w}{\partial t}+2\rho_f U\frac{\partial^2 w}{\partial t\,\partial x}=0 \tag{1}$$

In literature of fluid-structure interaction mechanics, where fluid induced vibrations are studied, Eqn. (1) is often non-dimensionalized as

$$\frac{\partial^4 \bar{W}}{\partial \xi^4}+\bar{k}_0\bar{W}+u^2\frac{\partial^2 \bar{W}}{\partial \xi^2}+\frac{\partial^2 \bar{W}}{\partial \tau^2}+\bar{\mu}\frac{\partial \bar{W}}{\partial \tau}+2\sqrt{\beta}u\frac{\partial^2 \bar{W}}{\partial \xi\partial \tau}=0 \tag{2}$$

where

$$v=UL\sqrt{\frac{\rho_f}{EI}};\ \beta=\frac{\rho_f}{\rho_p+\rho_f};\ \tau=\frac{t}{L^2}\sqrt{\frac{EI}{\rho_p+\rho_f}};\ \xi=\frac{x}{L};\bar{W}=\frac{w}{L};\ \bar{\mu}=\frac{\mu L^4}{EI\,\tau};\ \bar{k}_0=\frac{k_0 L^4}{EI}$$

whereas for the present study the dimensionless form is given by

$$\frac{\partial^4 \bar{W}}{\partial \bar{x}^4}+\bar{k}_0\bar{W}+\zeta_f\bar{U}^2\frac{\partial^2 \bar{W}}{\partial \bar{x}^2}+\left(1+\zeta_f\right)\frac{\partial^2 \bar{W}}{\partial \bar{t}^2}+\bar{\mu}\frac{\partial \bar{W}}{\partial \bar{t}}+2\zeta_f\bar{U}\frac{\partial^2 \bar{W}}{\partial \bar{t}\partial \bar{x}}=0 \tag{3}$$

where

$$\tau=L^2\sqrt{\frac{\rho_s}{EI}};\bar{W}=\frac{w}{L};\bar{x}=\frac{x}{L};\bar{t}=\frac{t}{\tau};\bar{U}=UL\sqrt{\frac{\rho_s}{EI}};\ \zeta_f=\frac{\rho_f}{\rho_s};\ \bar{k}_0=\frac{k_0 L^4}{EI};\ \bar{\mu}=\frac{\mu L^2}{\sqrt{\rho_s EI}}$$

The term $\frac{\partial^4 \bar{W}}{\partial \bar{x}^4}$ represents the acceleration due to the restoring force acting on the pipe arising from flexural bending. The components $\bar{k}_0\bar{W}\ and\ \bar{\mu}\frac{\partial \bar{W}}{\partial \bar{t}}$ depict the forces that emanate from the foundation stiffness and damping respectively. Whilst $\zeta_f\bar{U}^2\frac{\partial^2 \bar{W}}{\partial \bar{x}^2}$ is the acceleration term from the centrifugal force due to the internal flow in the deflected pipe. The component $(1+\zeta_f)\frac{\partial^2 \bar{W}}{\partial \bar{t}^2}$ is the acceleration due to the inertia force on the pipe. The term $2\zeta_f\bar{U}\frac{\partial^2 \bar{W}}{\partial \bar{t}\,\partial \bar{x}}$ represents the Coriolis acceleration as a result of internal fluid flow with velocity $\bar{U}$ relative to the pipe motion. For comparison purposes:

Case 1: We expect that if the pipeline segment is conveying a fluid and an eventual situation calls for the valve to be closed or the pump/compressor shut-off, then an entrainment fluid - be it hot, cold, pressurized or otherwise - will be trapped in the pipe. When the flow velocity $\bar{U}=0$, and Eqn. (2) – based on the non-dimensionalization method in literature will become

$$\lim_{as\,\bar{U}\to 0}\left(\frac{\partial^4 \bar{W}}{\partial \xi^4}+\bar{k}_0\bar{W}+u^2\frac{\partial^2 \bar{W}}{\partial \xi^2}+\frac{\partial^2 \bar{W}}{\partial \tau^2}+\bar{\mu}\frac{\partial \bar{W}}{\partial \tau}+2\sqrt{\beta}u\frac{\partial^2 \bar{W}}{\partial \xi\partial \tau}\right)=0$$

That is,

$$\frac{\partial^4 \bar{W}}{\partial \xi^4}+\frac{\partial^2 \bar{W}}{\partial \tau^2}+\bar{\mu}\frac{\partial \bar{W}}{\partial \tau}+\bar{k}_0\bar{W}=0 \tag{4}$$

leading to

$$\Omega_n = \frac{1}{2}\left\{-\bar{\mu} \pm \sqrt{\bar{\mu}^2 - 4\left(\lambda^2 + k_0\right)}\right\} \quad \forall \lambda = n\pi$$

which shows that, there is no fluid inside the pipe if the flow velocity is zero. This is not to be so. However, considering Eqn. (3) – based on this paper's dimensionless method – with $\bar{U} = 0$, it becomes

$$\lim_{as\,\bar{U} \to 0}\left(\frac{\partial^4 \bar{W}}{\partial \bar{x}^4} + \bar{k}_0 \bar{W} + \zeta_f \bar{U}^2 \frac{\partial^2 \bar{W}}{\partial \bar{x}^2} + 2\zeta_f \bar{U}\frac{\partial^2 \bar{W}}{\partial \bar{x}\,\partial \bar{t}} + \bar{\mu}\frac{\partial \bar{W}}{\partial \bar{t}} + \left(1+\zeta_f\right)\frac{\partial^2 \bar{W}}{\partial \bar{t}^2}\right)$$

That is,

3. $$\frac{\partial^4 \bar{W}}{\partial \bar{x}^4} + \bar{k}_0 \bar{W} + \left(1+\zeta_f\right)\frac{\partial^2 \bar{W}}{\partial \bar{t}^2} + \bar{\mu}\frac{\partial \bar{W}}{\partial \bar{t}} = 0 \tag{5}$$

Leading to,

$$\Omega_n = \frac{1}{2\left(1+\zeta_f\right)}\left\{-\bar{\mu} \pm \sqrt{\bar{\mu}^2 - 4\left(1+\zeta_f\right)\left(\lambda^2 + k_0\right)}\right\} \quad \forall \lambda = \mathrm{n}\pi$$

Revealing that, the system's vibration, configuration and response are strongly affected by the entrainment fluid in the pipe.

Case 2: If there is no fluid in the pipe, i.e. $\zeta_f = \beta = 0$, then Eqns. (2) and (3) respectively become

$$\lim_{as\,\beta \to 0}\left(\frac{\partial^4 \bar{W}}{\partial \xi^4} + \bar{k}_0 \bar{W} + u^2 \frac{\partial^2 \bar{W}}{\partial \xi^2} + \frac{\partial^2 \bar{W}}{\partial \tau^2} + \bar{\mu}\frac{\partial \bar{W}}{\partial \tau} + 2\sqrt{\beta}u\frac{\partial^2 \bar{W}}{\partial \xi \partial \tau}\right)$$

i.e. $$\frac{\partial^4 \bar{W}}{\partial \xi^4} + u^2 \frac{\partial^2 \bar{W}}{\partial \xi^2} + \frac{\partial^2 \bar{W}}{\partial \tau^2} + \bar{\mu}\frac{\partial \bar{W}}{\partial \tau} + \bar{k}_0 \bar{W} = 0 \tag{6}$$

Leading to,

$$\Omega_n = \frac{1}{2}\left\{-\bar{\mu} \pm \sqrt{\bar{\mu}^2 - 4\left(\lambda^4 - \lambda^2 u^2 + k_0\right)}\right\} \forall \lambda = \mathrm{n}\pi$$

and

$$\lim_{as\,\zeta_f \to 0}\left(\frac{\partial^4 \bar{W}}{\partial \bar{x}^4} + \bar{k}_0 \bar{W} + \zeta_f \bar{U}^2 \frac{\partial^2 \bar{W}}{\partial \bar{x}^2} + 2\zeta_f \bar{U}\frac{\partial^2 \bar{W}}{\partial \bar{x}\,\partial \bar{t}} + \bar{\mu}\frac{\partial \bar{W}}{\partial \bar{t}} + \left(1+\zeta_f\right)\frac{\partial^2 \bar{W}}{\partial \bar{t}^2}\right)$$

$$\frac{\partial^4 \bar{W}}{\partial \bar{x}^4} + \bar{k}_0 \bar{W} + \left(1+\zeta_f\right)\frac{\partial^2 \bar{W}}{\partial \bar{t}^2} + \bar{\mu}\frac{\partial \bar{W}}{\partial \bar{t}} = 0 \tag{7}$$

The literature method (Eqn. (6)) is showing that when no fluid is present in the pipe, there is still an internal flow velocity. This is not possible and is likely a fundamental error in physics. However, Eqn. (7) shows that the restoring and the inertial accelerations in dimensionless form are the balancing vectors.

Case 3: We now examine the governing equation (1) in its original form, that is, in its dimensional state; such that when $U = 0$, it becomes

$$EI\frac{\partial^4 w}{\partial x^4} + k_0 w + \left(\rho_p + \rho_f\right)\frac{\partial^2 w}{\partial t^2} + \mu\frac{\partial w}{\partial t} = 0 \tag{8}$$

Leading to,

$$\Omega_n = \frac{1}{2\rho_p\left(1+\zeta_f\right)}\left\{-\mu \pm \sqrt{\mu^2 + 4\rho_p\left(1+\zeta_f\right)\left(EI\left(\lambda/L\right)^4 + k_0\right)}\right\} \quad \forall \lambda = n\pi$$

and when there is no fluid in the pipe i.e. $\rho_f = 0$

$$EI\frac{\partial^4 w}{\partial x^4} + k_0 w + \rho_p \frac{\partial^2 w}{\partial t^2} + \mu\frac{\partial w}{\partial t} = 0 \tag{9}$$

Leading to,

$$\Omega_n = \frac{1}{2\rho_p}\left\{-\mu \pm 4\rho_p\left(EI\left(\lambda/L\right)^4 + k_0\right)\right\}\ \forall\lambda = n\pi$$

It is confirmed that Eqn. (8) is similar to Eqn. (5), demonstrating that the natural frequency is dependent on the mass or density of fluid flowing in the pipeline. We next define the following Fourier complex integral transforms Jeffrey [21] and Wrede & Spiegel [21], namely:

$$\begin{pmatrix} F\left\{\bar{W}\left(\bar{x},\bar{t}\right)\right\} = \dfrac{1}{\sqrt{2\pi}}\displaystyle\int_{-\infty}^{\infty} e^{-i\lambda x}\bar{W}\left(\bar{x},\bar{t}\right)d\bar{x} = \bar{W}\left(\lambda,\bar{t}\right); \\ F^{-1}\left\{\bar{W}\left(\lambda,\bar{t}\right)\right\} = \dfrac{1}{\sqrt{2\pi}}\displaystyle\int_{-\infty}^{\infty} e^{i\lambda\bar{x}}\bar{W}\left(\lambda,\bar{t}\right)d\lambda = \bar{W}\left(\bar{x},\bar{t}\right) \end{pmatrix} \tag{10}$$

where in this case

$$F\left(\bar{x},\bar{t}\right) = \begin{cases} 0 & when\ -\infty \le \bar{x} < 0 \\ \bar{W}\left(\bar{x},\bar{t}\right) & when\ 0 \le \bar{x} \le 1 \\ 0 & when\ 1 < \bar{x} \le \infty \end{cases}$$

On applying the Fourier transform on Eqn. (3) gives;

$$\frac{d^2\bar{W}^F}{d\bar{t}^2} + \frac{i\left(2\lambda\zeta_f\bar{U} - i\bar{\mu}\right)}{\left(1+\zeta_f\right)}\frac{d\bar{W}^F}{d\bar{t}} + \frac{\left(\lambda^4 - \zeta_f\bar{U}^2\lambda^2 + \bar{k}_0\right)}{\left(1+\zeta_f\right)}\bar{W}^F = \frac{\left(-\bar{W}_{\bar{x}\bar{x}\bar{x}}\left(0,\bar{t}\right)e^{-i\lambda\bar{x}}\Big|_0^1 + \left(\lambda^2 - \zeta_f U^2\right)\bar{W}_{\bar{x}}\left(0,\bar{t}\right)e^{-i\lambda\bar{x}}\Big|_0^1\right)}{\left(1+\zeta_f\right)} \tag{11}$$

Subject to simple supports at both ends, i.e.,

$$\begin{pmatrix} \bar{W}\left(0,t\right) = \bar{W}_{xx}\left(0,t\right) = 0 \\ \bar{W}\left(1,t\right) = \bar{W}_{xx}\left(1,t\right) = 0 \end{pmatrix}$$

In conjunction with the following conditions

$$\frac{d\bar{W}\left(0,t\right)}{d\bar{t}} = \frac{d\bar{W}\left(1,t\right)}{d\bar{t}} = 0$$

Since the resultant equation is an in-homogeneous second order ordinary differential equation in the transform plane, we seek the solution in the next subsection.

3. Complex natural frequencies

In this subsection, our interest is to compute the complex natural frequencies from the solution $W^F\left(\lambda,\bar{t}\right)$ in Eqn. (11). A closed form solution can be obtained via a complimentary equation of the form;

$$W^F\left(\lambda,\bar{t}\right) = Ae^{s\bar{t}} \tag{12}$$

leading to the following characteristic equation, namely;

$$\left(s^2 + i\left(\frac{\left(2\lambda\zeta_f\bar{U} - i\bar{\mu}\right)}{\left(1+\zeta_f\right)}\right)s + \frac{\left(\lambda^4 - \zeta_f\bar{U}^2\lambda^2 + \bar{k}_0\right)}{\left(1+\zeta_f\right)}\right)Ae^{s\bar{t}} = 0$$

to give complex conjugate pairs of the forms;

$$\Omega_{1,2} = -\left(\frac{2\lambda\zeta_f\bar{U} - i\bar{\mu}}{2\left(1+\zeta_f\right)}\right) \mp \sqrt{\left(\frac{2\lambda\zeta_f\bar{U} - i\bar{\mu}}{2\left(1+\zeta_f\right)}\right)^2 + \frac{\left(\lambda^4 - \zeta_f\bar{U}^2\lambda^2 + \bar{k}_0\right)}{\left(1+\zeta_f\right)}} \tag{13}$$

In order to separate the Coriolis and damping forces from the complex natural frequencies, we introduce the expression

$$\Omega_{cd} = \left(\frac{2\lambda\zeta_f\bar{U} - i\bar{\mu}}{2\left(1+\zeta_f\right)}\right) \tag{14}$$

into Eqns. (14). On comparing these equations with the Coriolis frequency, the relative frequencies are;

$$\Omega_{1,2} = -\Omega_n\left(\left(\xi - i\,\frac{\bar{\mu}_c}{2}\right) \pm \sqrt{1+\left(\xi - \frac{i\,\bar{\mu}_c}{2}\right)^2}\right) \tag{15}$$

where

$$\xi = \frac{\Omega_{cor}}{\Omega_n};\ \bar{\mu}_c = \frac{\bar{\mu}}{\Omega_n}$$

The algebraic product of the foregoing gives

$$\Omega_1 \times \Omega_2 = \Omega_n{}^2 = \frac{\left(\lambda^4 - \zeta_f \bar{U}^2\lambda^2 + \bar{k}_0\right)}{\left(1+\zeta_f\right)} \tag{16}$$

The observation from relation (16) is that the rational natural frequency of the system on the real axis is independent of the Coriolis and damping forces, a generalized equation can readily be conjured as;

$$\Omega_n^2 = \Omega_0^2\left(1 - \frac{U^2}{U_{cr}^2}\right) \tag{17}$$

to express the rational natural frequency as a function of critical flow velocity. As $U = U_{cr}$, the rational natural frequency tends to zero, i.e. $\Omega_n \to 0$, the system instabilities develop.

3.1 Dynamic Response Analysis

For the case of a pipe segment that is subjected to a uniformly distributed load of the form f Newton per unit length is as illustrated in Figure 2 below. The deflection function for the static configuration is given as, (see Nash, 1977);

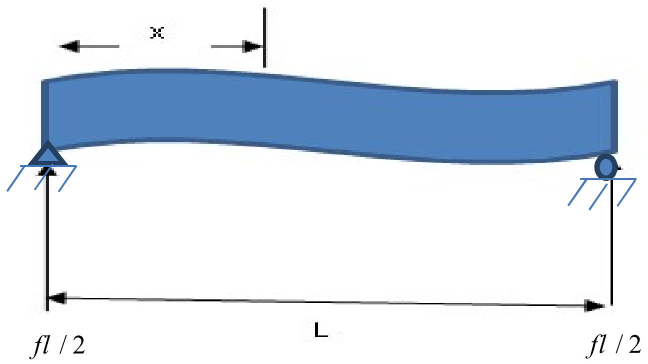

Fig. 2. Simply supported S-shape beam with distributed load

$$\bar{W} = \beta_f\left(1+\zeta_f\right)\left(\frac{\bar{x}^4}{6} - \frac{\bar{x}^5}{4} + \frac{2\bar{x}^6}{15} - \frac{\bar{x}^7}{42} - \frac{11\bar{x}}{420}\right) \tag{18}$$

where

$\beta_f = \dfrac{m_p L}{2EI}$, with m_p as the mass of pipe and the complete solution is as follows;

$$\bar{W}^F\left(\lambda,\bar{t}\right) = A\left(\lambda\right)e^{-i\Omega_1\bar{t}} + B\left(\lambda\right)e^{-i\Omega_2\bar{t}} + \frac{J\left(\lambda\right)}{\left(\lambda^4 - \zeta_f\bar{U}^2\lambda^2 + \bar{k}_0\right)} \tag{19}$$

where

$$J\left(\lambda\right) = \left(-\bar{W}_{\bar{x}\bar{x}\bar{x}}\left(0,0\right)e^{-i\lambda\bar{x}}\Big|_0^1 + \left(\lambda^2 - \zeta_f U^2\right)\bar{W}_{\bar{x}}\left(0,0\right)e^{-i\lambda\bar{x}}\Big|_0^1\right) \tag{20}$$

By applying the initial pipe velocity at the support ends, we solve for $A\left(\lambda\right), B\left(\lambda\right)$ *and* $\bar{W}\left(\lambda,\bar{t}\right)$ as follows;

$$A(\lambda)=-\frac{1}{\Omega_1-\Omega_2}\left(\Omega_1 H(\lambda)-\frac{\Omega_2 J(\lambda)}{\Omega_n^2(1+\zeta_f)}\right)-\frac{2\Omega_{cor}}{\Omega_1-\Omega_2}H(\lambda) \tag{21}$$

$$B(\lambda)=\frac{2\Omega_{cor}}{\Omega_1-\Omega_2}H(\lambda)+\frac{1}{\Omega_1-\Omega_2}\left(\Omega_2 H(\lambda)-\frac{\Omega_1 J(\lambda)}{\Omega_n^2(1+\zeta_f)}\right) \tag{22}$$

where

$$H(\lambda)=\int_0^1 \bar{W}(\bar{x},0)e^{-i\lambda\bar{x}}d\bar{x}=\beta_f(1+\zeta_f)\int_0^1\left(\frac{\bar{x}^4}{6}-\frac{\bar{x}^5}{4}+\frac{2\bar{x}^6}{15}-\frac{\bar{x}^7}{42}-\frac{11\bar{x}}{420}\right)e^{-i\lambda\bar{x}}d\bar{x} \tag{23}$$

$$\Omega_n^2=\frac{\lambda^4-\lambda^2\bar{U}^2\zeta_f+\bar{k}_0}{(1+\zeta_f)} \tag{24}$$

The response in the Fourier domain is given as

$$\bar{W}^F(\lambda,\bar{t})=-\frac{\Omega_2 e^{-i\Omega_2\bar{t}}-\Omega_1 e^{-i\Omega_1\bar{t}}-2\Omega_{cd}\left(e^{-i\Omega_1\bar{t}}-e^{-i\Omega_2\bar{t}}\right)}{\Omega_1-\Omega_2}H(\lambda,0) -\frac{\left(\Omega_1 e^{-i\Omega_2\bar{t}}-\Omega_2 e^{-i\Omega_1\bar{t}}\right)-(\Omega_1-\Omega_2)}{(\Omega_1-\Omega_2)(1+\zeta_f)}\frac{J(\lambda)}{\Omega_n^2} \tag{25}$$

Recalling the inverse Fourier transform namely (see ref. [20]);

$$\bar{W}(\bar{x},\bar{t})=\frac{1}{\sqrt{2\pi}}\int_{-\infty}^{\infty}\bar{W}(\lambda,\bar{t})e^{i\lambda\bar{x}}d\lambda \tag{26}$$

in conjunction with Eqns. (20, 23, 25 and 26) gives;

$$\bar{W}(\bar{x},\bar{t})=\beta_f(1+\zeta_f)\frac{\begin{pmatrix}\Omega_2 e^{-i\Omega_2\bar{t}}-\Omega_1 e^{-i\Omega_1\bar{t}}\\ -2\Omega_{cd}\left(e^{-i\Omega_1\bar{t}}-e^{-i\Omega_2\bar{t}}\right)\end{pmatrix}\left(\frac{\bar{x}^4}{6}-\frac{\bar{x}^5}{4}+\frac{2\bar{x}^6}{15}-\frac{\bar{x}^7}{42}-\frac{11\bar{x}}{420}\right)}{(\Omega_2-\Omega_1)} -\Im^{-1}\{\Lambda J(\lambda)\} \tag{27}$$

Next, on applying the initial conditions $\dot{\bar{W}}(0,\bar{t})=\dot{\bar{W}}(1,\bar{t})=0$, the second term in Eqn. (27) becomes

$$\Im^{-1}\{\Lambda J(\lambda)\}=-\frac{11\beta_f(1+\zeta_f)}{420}\int_{-\infty}^{\infty}\left(\frac{\Omega_2 e^{-i\Omega_1\bar{t}}-\Omega_1 e^{-i\Omega_2\bar{t}}-(\Omega_2-\Omega_1)}{\Omega_n^2(\Omega_2-\Omega_1)}\right)\times\left(\lambda^2-\bar{U}^2\zeta_f\right)\left(e^{-i\lambda}-1\right)e^{i\lambda\bar{x}}d\lambda \tag{28}$$

and simplified to the form;

$$\Im^{-1}\{\Lambda J(\lambda)\}=-\frac{11\beta_f(1+\zeta_f)}{420}\int_{-\infty}^{\infty}\frac{\left(\Omega_2\left(e^{-i\Omega_1\bar{t}}-1\right)-\Omega_1\left(e^{-i\Omega_2\bar{t}}-1\right)\right)}{(\Omega_2-\Omega_1)}\times\frac{\left(\lambda^2-\bar{U}^2\zeta_f\right)\left(e^{-i\lambda}-1\right)e^{i\lambda\bar{x}}}{\left(\lambda-\sqrt{\eta}\right)\left(\lambda+\sqrt{\eta}\right)}d\lambda$$

where

$$\eta=\left(\frac{\bar{U}^2\zeta_f}{2}\pm\sqrt{\frac{\bar{U}^4\zeta_f^2}{4}-k_0}\right)^{1/2}$$

On applying residue theory with $\lambda=\pm\sqrt{\eta_2}$, $\Im^{-1}\{\Lambda J(\lambda)\}=0$ i.e., the system becomes identically zero; but with $\lambda=\pm\sqrt{\eta_2}$, the following can be deduced, namely;

$$\Im^{-1}\{\Lambda J(\lambda)\}=-\frac{11\beta_f(1+\zeta_f)}{420}\frac{\left(\Omega_2\left(e^{-i\Omega_1\bar{t}}-1\right)-\Omega_1\left(e^{-i\Omega_2\bar{t}}-1\right)\right)}{(\Omega_2-\Omega_1)}\times\frac{\left(\eta-\bar{U}^2\zeta_f\right)}{2\sqrt{\eta}}\left(e^{-i\sqrt{\eta_1}(1-\bar{x})}-e^{i\sqrt{\eta_1}(1-\bar{x})}-\left(e^{i\sqrt{\eta_1}\bar{x}}-e^{-i\sqrt{\eta_1}\bar{x}}\right)\right)$$

resulting to

$$\Im^{-1}\left\{\Lambda J\left(\lambda\right)\right\}=\frac{11\beta_f\left(1+\zeta_f\right)\left(\eta-\bar{U}^2\zeta_f\right)}{420\sqrt{\eta_1}}\left(\begin{array}{c}\dfrac{\left(\Omega_2\left(e^{-i\Omega_1\bar{t}}-1\right)-\Omega_1\left(e^{-i\Omega_2\bar{t}}-1\right)\right)}{\left(\Omega_2-\Omega_1\right)}\\ \times\left(\sin\sqrt{\eta_1}\left(1-\bar{x}\right)+\sin\sqrt{\eta_1}\bar{x}\right)\end{array}\right) \tag{29}$$

We can infer the conditions at $\bar{x}=0\ or\ 1$ such that $\Im^{-1}\left\{\Lambda J\left(\lambda\right)\right\}=0$, since

$$\frac{11\beta_f\left(1+\zeta_f\right)\left(\eta-\bar{U}^2\zeta_f\right)}{420\sqrt{\eta}}\frac{\left(\Omega_2\left(e^{-i\Omega_1\bar{t}}-1\right)-\Omega_1\left(e^{-i\Omega_2\bar{t}}-1\right)\right)}{\left(\Omega_2-\Omega_1\right)}\neq 0$$

to deduce that

$$\sin\sqrt{\eta}=0$$

leads to the following condition viz.

$$\sqrt{\eta}=n\pi\Rightarrow\lambda^2=n^2\pi^2=\left(\frac{\bar{U}^2\zeta_f}{2}\pm\sqrt{\frac{\bar{U}^4\zeta_f^2-4k_0}{4}}\right)$$

From Eqn. (26), we have

$$\Omega_n^2=\lambda^4-\lambda^2\bar{U}^2\zeta_f+k_0=0$$

but letting $\eta=\lambda^2$ leads to

$$\eta^2-\eta\bar{U}^2\zeta_f+k_0=0$$

Since from Eqn. (27) $\sqrt{\eta}=n\pi$ and consequently $\lambda^2=n^2\pi^2$, then

$$n^4\pi^4-n^2\pi^2\bar{U}^2\zeta_f+k_0=0$$

Solving to give

$$\bar{U}_{cr}=\frac{n\pi}{\sqrt{\zeta_f}}\sqrt{\left(1+\frac{k_0}{n^4\pi^4}\right)}$$

That is,

$$\bar{U}_{cr}=\frac{n\pi}{\sqrt{\zeta_f}}\left(1+\frac{k_0}{2n^4\pi^4}+\frac{1}{8}\left(\frac{k_0}{n^4\pi^4}\right)^2+\cdots\right) \tag{30a}$$

Leading approximately to

$$\bar{U}_{cr}=\frac{n\pi}{\sqrt{\zeta_f}}+\frac{k_0}{2n^3\pi^3\sqrt{\zeta_f}} \tag{30b}$$

As the foundation stiffness k_0 tends to zero, the critical velocity of flow reverts to the earlier result, viz.

$$\bar{U}_{cr}=\frac{n\pi}{\sqrt{\zeta_f}}\quad\forall n=1,2,... \tag{31}$$

Using Eqns. (26) and (29) on Eqn. (25), the dynamic response of the system follows as;

$$\bar{W}\left(\bar{x},\bar{t}\right)=\frac{\beta_f\left(1+\zeta_f\right)}{420}\left(\begin{array}{c}\dfrac{\left(\Omega_2e^{-i\Omega_2\bar{t}}-\Omega_1e^{-i\Omega_1\bar{t}}-2\Omega_{cd}\left(e^{-i\Omega_1\bar{t}}-e^{-i\Omega_2\bar{t}}\right)\right)}{\left(\Omega_2-\Omega_1\right)}\\ \cdot\bar{x}\left(70\bar{x}^{-3}-105\bar{x}^{-4}+56\bar{x}^{-5}-10\bar{x}^{-6}-11\right)\\ +\dfrac{11\left(\bar{U}_{cr}^2-\bar{U}^2\right)\zeta_f}{n\pi}\dfrac{\left(\Omega_2\left(e^{-i\Omega_1\bar{t}}-1\right)-\Omega_1\left(e^{-i\Omega_2\bar{t}}-1\right)\right)}{\left(\Omega_2-\Omega_1\right)}\\ \cdot\left(\sin n\pi\left(1-\bar{x}\right)+\sin n\pi\bar{x}\right)\end{array}\right) \tag{32}$$

and further reduces to the following form

$$\bar{W}\left(\bar{x},\bar{t}\right)=\frac{\beta_f\left(1+\zeta_f\right)}{420}\left(\begin{array}{l}\dfrac{\left(\Omega_2 e^{-i\Omega_2\bar{t}}-\Omega_1 e^{-i\Omega_1\bar{t}}-2\Omega_{cd}\left(e^{-i\Omega_1\bar{t}}-e^{-i\Omega_2\bar{t}}\right)\right)}{\left(\Omega_2-\Omega_1\right)}\\ \times\bar{x}\left(70\bar{x}^3-105\bar{x}^4+56\bar{x}^5-10\bar{x}^6-11\right)\\ +\dfrac{11\left(\bar{U}_{cr}^2-\bar{U}^2\right)\zeta_f}{n\pi}\dfrac{\left(\Omega_2\left(e^{-i\Omega_1\bar{t}}-1\right)-\Omega_1\left(e^{-i\Omega_2\bar{t}}-1\right)\right)}{\left(\Omega_2-\Omega_1\right)}\\ \times\left(1-\left(-1\right)^{n+1}\right)\sin n\pi\bar{x}\end{array}\right) \tag{33}$$

where

$$\Omega_1=-\Omega_{cd}-\sqrt{\Omega_{cd}^2+\Omega_n^2}\quad \Omega_2=-\Omega_{cd}+\sqrt{\Omega_{cd}^2+\Omega_n^2}$$

$$\Omega_{cd}=\left(\frac{2\lambda\zeta_f\bar{U}-i\upsilon\bar{\mu}}{2\left(1+\zeta_f\right)}\right)\quad \Omega_n=\sqrt{\frac{\lambda^4-\zeta_f\bar{U}^2\lambda^2+\bar{k}_0}{1+\zeta_f}}$$

$$\eta=\lambda^2=\left(\frac{\bar{U}^2\zeta_f}{2}\pm\sqrt{\frac{\bar{U}^4\zeta_f^2}{4}-k_0}\right)$$

We shall comparing Eqns. (16) and (17) to examine the following three scenarios namely; at the critical, sub-critical and post-critical flow points. Firstly;

$$1-\Gamma^2=\frac{\lambda^4-\zeta_f\bar{U}^2\lambda^2+\bar{k}_0}{\Omega_0^2\left(1+\zeta_f\right)} \tag{34}$$

where

$$\Gamma^2=\frac{U^2}{U_{cr}^2} \tag{35}$$

Next, the arguments for computing the residues as in Eqn. (29) are $\lambda=\pm\bar{U}\sqrt{\zeta_f}$ and possible only when $\left(\lambda-\sqrt{\eta}\right)\left(\lambda+\sqrt{\eta}\right)=0$, where $\eta=\left(\frac{\bar{U}^2\zeta_f}{2}\pm\sqrt{\frac{\bar{U}^4\zeta_f^2}{4}-k_0}\right)$. From Eqn. (31) at the critical point, i.e. $1-\Gamma^2=0$ (where divergence occurs), Eqn. (31) becomes

$$\bar{U}=\bar{U}_{cr} \tag{36}$$

and, at the sub-critical points where $\Gamma<1$, the internal flow velocity takes the form

$$\bar{U}<\bar{U}_{cr} \tag{37}$$

whereas, at the post-critical points i.e. when $\Gamma>1$, the flow velocity is such that

$$\bar{U}>\bar{U}_{cr} \tag{38}$$

These scenarios describe the dynamic behaviors of the pipeline segment with fluid transmission at various flow velocities.

3.2 Logarithmic Decrement Analysis

All real systems dissipate energy when they vibrate. If the damping is significant, its effects must be included in the analysis, particularly when the amplitude of vibration is required. Energy is dissipated by frictional effects, as in the case of the pipe segment system resting on the visco-elastic foundation. Common types of damping are viscous, dry friction and hysteretic, etc. A convenient way of determining the damping in a system is to measure the rate of decay of oscillation. Consequently the logarithmic decrement, arising from the ratio of any two successive amplitudes in the same direction can be applied. The same logarithmic damping coefficient can be used as a measure of the damping capacity of a structure. Here, the effect of the length between two supporting ends on the fluid-conveying pipeline damping capacity is particularly noted and investigated. The characteristics of the decrement with the flow velocity and time are to be especially studied.

Recall from Eqns. (11), (14) and (15) that the homogeneous form of the governing equation can be written as

$$\frac{d^2\bar{W}^F}{d\bar{t}^2}+2\Omega_{cd}\frac{d\bar{W}^F}{d\bar{t}}+\Omega_n^2\bar{W}^F=0 \tag{39}$$

Using $\bar{W}^F=e^{\Omega_n\bar{t}}\cdot\bar{Z}$ transforms Eqn. (39) to the following

$$\frac{d^2\bar{Z}}{d\bar{t}^2}+\bar{\mu}_v{}^2\bar{Z}=0 \tag{40}$$

where

$$\bar{\mu}_v{}^2=\Omega_n^2-\Omega_{cd}^2$$

since, the solution to Eqn. (40) is $\bar{Z}=A\cos\left(\bar{\mu}\bar{t}+\varepsilon\right)$, then the solution to Eqn. (39) can be expressed as

$$\bar{W}^F=e^{-\Omega_{cd}\bar{t}}\cdot A\cos\left(\bar{\mu}_v\bar{t}+\varepsilon\right) \tag{41}$$

This may represent typical simple harmonic motion, with its amplitude diminishing exponentially to zero as the time $\bar{t}$ increases. Now, if we start measuring the motion when the phase angle $\varepsilon=0$, i.e. $\bar{W}^F=A$, then

$$\bar{W}^F=e^{-\Omega_{cd}\bar{t}}\cdot A\cos\bar{\mu}_v\bar{t} \tag{42}$$

As depicted by the displacement-time curves shown in Figures 3-5. When $\bar{W}^F=0$, then $\cos\bar{\mu}_v\bar{t}=0$ i.e. $\bar{\mu}_v\bar{t}=\left(2n-1\right)\pi/2$, and when $d\bar{W}^F/d\bar{t}=0$, $\tan\bar{\mu}_v\bar{t}=-\Omega_{cd}/\bar{\mu}_v$, leading to two successive amplitudes at $n=k$ and $n=k+1$ are compared to give the Amplitude Reduction Ratio (ARR) of the system as [23-24]

$$ARR=\frac{\bar{W}^F_{\tau+1}}{\bar{W}^F_{\tau}}=-e^{-\Omega_{cd}\left(\bar{t}_{\tau+1}-\bar{t}_{\tau}\right)}=-e^{-\frac{\Omega_{cd}\pi}{\bar{\mu}_v}} \tag{43}$$

Now, from the given ARR, the logarithmic decrement of the motion can then be deduced as

$$\ln\frac{\bar{W}^F_{\tau+1}}{\bar{W}^F_{\tau}}=\frac{2\Omega_{cd}\pi}{\sqrt{\Omega_n^2-\Omega_{cd}^2}} \tag{44}$$

Hence, from Eqn. (43) and for the fundamental mode, we write the logarithmic damping for the mid-position of the system is computed as;

$$\delta=\ln\left\{\frac{\bar{W}\left(\frac{1}{2},0\right)}{\bar{W}\left(\frac{1}{2},\bar{t}\right)}\right\}=\ln\frac{\left(\Omega_1-\Omega_2\right)}{\Omega_{cd}\left(e^{-i\Omega_1\bar{t}}-e^{-i\Omega_2\bar{t}}\right)-\left(\Omega_1e^{-i\Omega_1\bar{t}}-\Omega_2e^{-i\Omega_2\bar{t}}\right)} \tag{45}$$

where

$$\bar{W}\left(\frac{1}{2},0\right)=-\left(\frac{1}{2}\right)^3\frac{231\beta_f}{3360}\left(1+\zeta_f\right)$$

and

$$\bar{W}\left(\frac{1}{2},\bar{t}\right)=\left(\frac{1}{2}\right)^3\frac{231\beta_f}{3360}\left(1+\zeta_f\right)\left(\frac{\Omega_{cd}\left(e^{-i\Omega_2\bar{t}}-e^{-i\Omega_1\bar{t}}\right)-\left(\Omega_1e^{-i\Omega_1\bar{t}}-\Omega_2e^{-i\Omega_2\bar{t}}\right)}{\left(\Omega_2-\Omega_1\right)}\right)$$

Invariably for the next cycle the following ensues viz;

$$\delta=\ln\left\{\frac{\bar{W}\left(\frac{1}{2},\tau\right)}{\bar{W}\left(\frac{1}{2},\tau+1\right)}\right\}=\ln\frac{\Omega_{cd}\left(e^{-i\Omega_1\tau}-e^{-i\Omega_2\tau}\right)+\left(\Omega_2e^{-i\Omega_2\tau}-\Omega_1e^{-i\Omega_1\tau}\right)}{\Omega_{cd}\left(e^{-i\Omega_1(\tau+1)}-e^{-i\Omega_2(\tau+1)}\right)+\left(\Omega_2e^{-i\Omega_2(\tau+1)}-\Omega_1e^{-i\Omega_1(\tau+1)}\right)} \tag{46}$$

Recalling, the bending moment as

$$M=EI\frac{d^2\bar{W}\left(\bar{x},\bar{t}\right)}{d\bar{x}^2}$$

where

$$\frac{d^2\bar{W}\left(\bar{x},\bar{t}\right)}{d\bar{x}^2}=\beta_f\left(1+\zeta_f\right)\left(\frac{\left(e^{-i\Omega_1\bar{t}}-e^{-i\Omega_2\bar{t}}\right)+\left(\Omega_2e^{-i\Omega_2\bar{t}}-\Omega_1e^{-i\Omega_1\bar{t}}\right)}{\left(\Omega_2-\Omega_1\right)}\right)$$
$$\times\left(2\bar{x}^2-5\bar{x}^3+4\bar{x}^4-\bar{x}^5\right)$$

gives the strain energy of the structure as

$$U_1 = \int_0^{1/2} \frac{M^2}{2EI} d\bar{x} = \left\{ \beta_f \left(1+\zeta_f\right) \left(\frac{\Omega_{cd}\left(e^{-i\Omega_1\bar{t}} - e^{-i\Omega_2\bar{t}}\right) + \left(\Omega_2 e^{-i\Omega_2\bar{t}} - \Omega_1 e^{-i\Omega_1\bar{t}}\right)}{\left(\Omega_2 - \Omega_1\right)} \right) \right\}^2 \times \bar{x}^5 \left(\frac{4}{5} - \frac{10}{3}\bar{x} + \frac{41}{7}\bar{x}^2 - \frac{13}{2}\bar{x}^3 + \frac{26}{9}\bar{x}^4 - \frac{4}{5}\bar{x}^5 + \frac{1}{11}\bar{x}^6 \right) \tag{47}$$

i.e. when $\bar{x} = 0.5$,

$$U_1 = \left(\frac{1}{2}\right)^5 (0.101) \left\{ \beta_f \left(1+\zeta_f\right) \left(\frac{\Omega_{cd}\left(e^{-i\Omega_1\bar{t}} - e^{-i\Omega_2\bar{t}}\right) + \left(\Omega_2 e^{-i\Omega_1\bar{t}} - \Omega_1 e^{-i\Omega_2\bar{t}}\right)}{\left(\Omega_2 - \Omega_1\right)} \right) \right\}^2$$

with other strain energies as;

$$U_2 = \frac{3EI\bar{W}^2}{2L^3} = \left(\frac{1}{2}\right)^2 \frac{1587EI}{(64)(313600)} \left\{ \begin{array}{l} \beta_f \left(1+\zeta_f\right) \\ \times \left(\dfrac{\Omega_{cd}\left(e^{-i\Omega_1\bar{t}} - e^{-i\Omega_2\bar{t}}\right) + \left(\Omega_2 e^{-i\Omega_2\bar{t}} - \Omega_1 e^{-i\Omega_1\bar{t}}\right)}{\left(\Omega_2 - \Omega_1\right)} \right) \end{array} \right\}^2 \tag{48}$$

and

$$\begin{aligned} U_3 &= K_{eq} \left\{ \bar{W}\left(\frac{1}{2}, \bar{t}\right) \right\}^2 = \Omega_n^2 \left\{ \bar{W}\left(\frac{1}{2}, \bar{t}\right) \right\}^2 \\ &= \left(\frac{1}{2}\right)^6 \frac{529\Omega_n^2}{(64)(313600)} \left\{ \beta_f \left(1+\zeta_f\right) \left(\frac{\Omega_{cd}\left(e^{-i\Omega_1\bar{t}} - e^{-i\Omega_2\bar{t}}\right) + \left(\Omega_2 e^{-i\Omega_2\bar{t}} - \Omega_1 e^{-i\Omega_1\bar{t}}\right)}{\left(\Omega_2 - \Omega_1\right)} \right) \right\}^2 \end{aligned} \tag{49}$$

Consequently, the total strain energy can be computed as

$$U = \left(\frac{1}{2}\right)^2 \left((0.101)\left(\frac{1}{2}\right)^3 + \frac{(1587)EI}{(64)(313600)} + \left(\frac{1}{2}\right)^4 \frac{529\Omega_n^2}{(64)(313600)} \right) \times \left\{ \beta_f \left(1+\zeta_f\right) \left(\frac{\Omega_{cd}\left(e^{-i\Omega_1\bar{t}} - e^{-i\Omega_2\bar{t}}\right) + \left(\Omega_2 e^{-i\Omega_1\bar{t}} - \Omega_1 e^{-i\Omega_2\bar{t}}\right)}{\left(\Omega_2 - \Omega_1\right)} \right) \right\}^2 \tag{50}$$

Whilst, the dissipation energy is obtained as follows;

$$\begin{aligned} D &= C_{eq} \left\{ \dot{\bar{W}}\left(\frac{1}{2}, \bar{t}\right) \right\}^2 = \Omega_{cd} \left\{ \dot{\bar{W}}\left(\frac{1}{2}, \bar{t}\right) \right\}^2 \\ &= i\left(\frac{1}{2}\right)^6 \frac{529\Omega_{cd}}{(64)(313600)} \left\{ \beta_f \left(1+\zeta_f\right) \left(\frac{\Omega_{cd}\left(\Omega_1 e^{-i\Omega_1\bar{t}} - \Omega_2 e^{-i\Omega_2\bar{t}}\right) - i\Omega_1\Omega_2\left(e^{-i\Omega_1\bar{t}} - e^{-i\Omega_2\bar{t}}\right)}{\left(\Omega_2 - \Omega_1\right)} \right) \right\}^2 \end{aligned} \tag{51}$$

In view of the foregoing, the logarithmic damping decrement Λ becomes

$$\Lambda = \frac{1}{2} \ln \left\{ 1 + \frac{D}{U_1 + U_2 + U_3} \right\} = \frac{1}{2} \ln \left\{ 1 + \frac{D}{U} \right\} \tag{52}$$

and computed as;

$$\Lambda = \frac{1}{2} \ln \left(1 + \frac{\Psi^2 \Omega_{cd}}{383.2 + 3EI + \Omega_n^2} \right) \tag{53}$$

where

$$\Psi = \frac{\left(\Omega_1 e^{-i\Omega_1\bar{t}} - \Omega_2 e^{-i\Omega_2\bar{t}}\right) - \dfrac{\Omega_1\Omega_2}{\Omega_{cd}}\left(e^{-i\Omega_1\bar{t}} - e^{-i\Omega_2\bar{t}}\right)}{\left(e^{-i\Omega_1\bar{t}} - e^{-i\Omega_2\bar{t}}\right) + \dfrac{\left(\Omega_2 e^{-i\Omega_1\bar{t}} - \Omega_1 e^{-i\Omega_2\bar{t}}\right)}{\Omega_{cd}}}$$

4 Analysis of Results and Discussion

The effect of viscoelastic foundation on the dynamic stability of the segment of a pipeline system conveying an incompressible fluid is the motivation for this study. A close observation of each of the Figures 3, 4 and 5 indicates progressive damping profiles for the dynamic response as functions of time. The amplitudes are exponentially diminishing for every successive beat. The damping effects are handled in Eqn. (42) as clearly shown in Figures 3-5. The tendency for the formation of beat phenomenon could be tied to fluid-pipe mass ratio in a manner that strongly illustrates an enhancing of the process with increasing fluid-pipe mass ratio. It is also clear that the system acted like coupled oscillators – one on the part of the combined damping and Coriolis forces, and the pipeline system as the second. In the characteristics, we observe that there are envelopments formed by the slow-moving frequency displacements over the fast-moving frequency response.

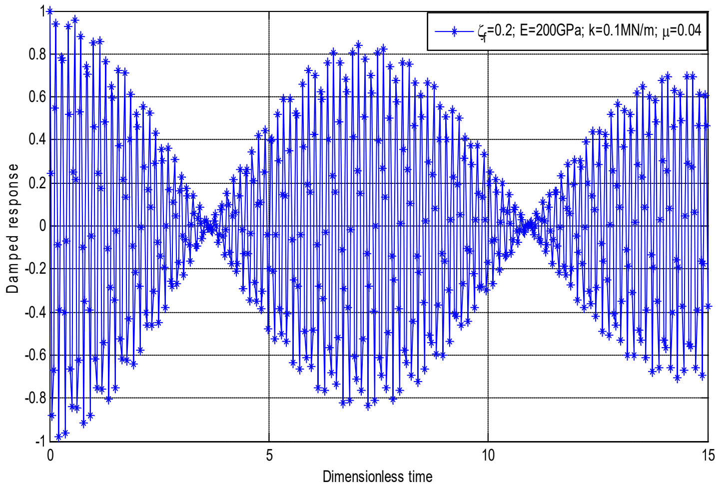

(a)

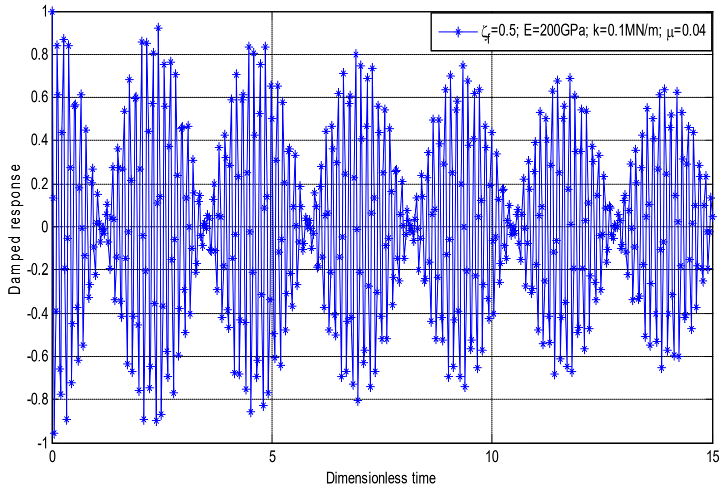

(b)

Fig. 3. Graph of $\overline{W}^F = e^{-\Omega_{cd}\bar{t}} \cos\sqrt{\left(\Omega_n^2 - \Omega_{cd}^2\right)}\,\bar{t}$ versus $\bar{t}$

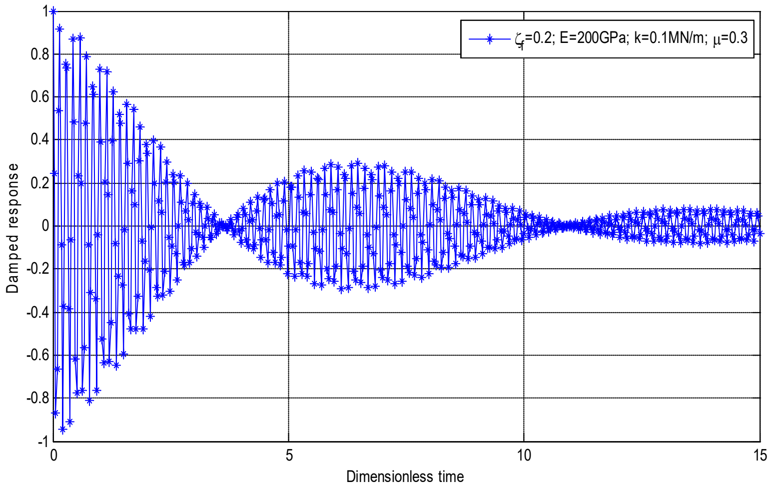

(a)

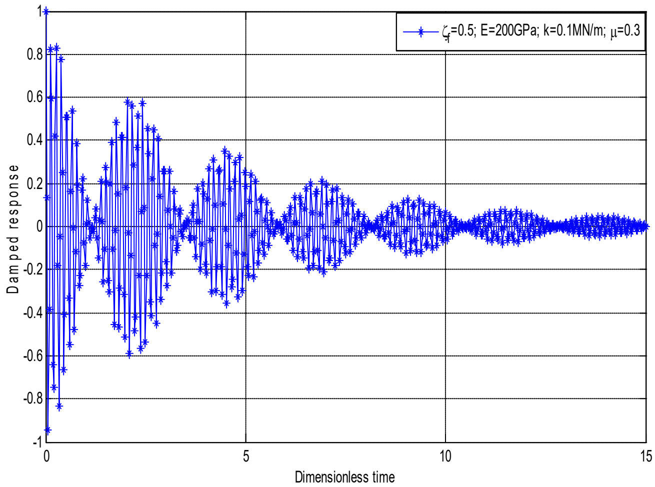

(b)

Fig. 4. Graph of $\overline{W}^F = e^{-\Omega_{cd}\bar{t}}\cos\sqrt{\left(\Omega_n^2 - \Omega_{cd}^2\right)}\,\bar{t}$ versus $\bar{t}$

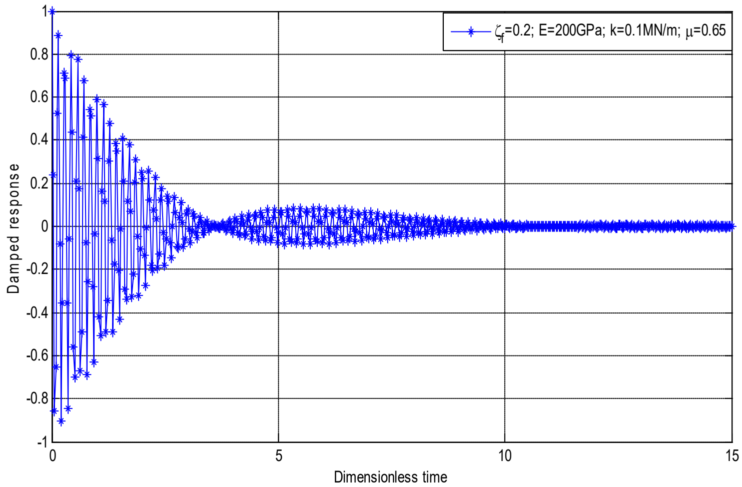

(a)

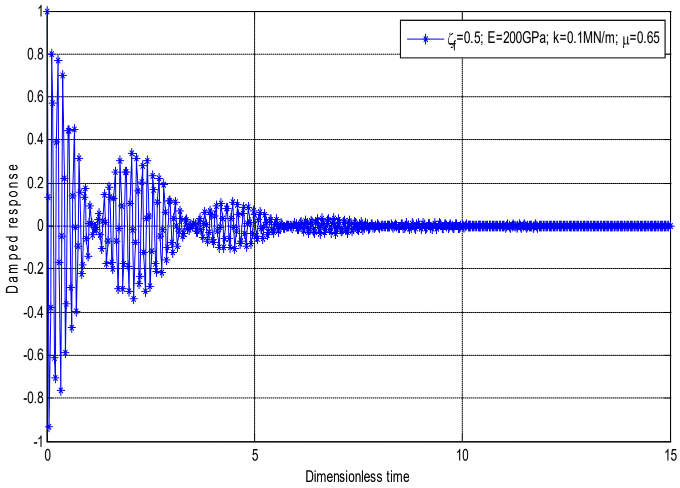

(b)

Fig. 5. Graph of $\bar{W}^F = e^{-\Omega_{cd}\bar{t}} \cos\sqrt{\left(\Omega_n^2 - \Omega_{cd}^2\right)}\,\bar{t}$ versus $\bar{t}$

The plots of the Amplitude Reduction Ratio (ARR) against the flow velocity show that increasing the fluid-pipe mass ratio and modal values strongly affected the response amplitude reduction as the flow velocity increases (Figures 6, 7). With smaller values of fluid-pipe mass ratio and modal values, ARR grew exponentially to maximum values at smaller flow velocities while further increase in flow velocities maintains almost constant peak values. Figures 8 and 9 illustrate the characteristics of ARR against the values of coefficient of friction as the fluid-pipe mass ratio and modal values are respectively altered. An effective control of the growing ARR vibration (oscillation) is observable as the coefficient of friction increases.

Figure 10 demonstrates ARR relationships with the fluid-pipe mass ratio. It readily shows that ARR increases steeply to the maximum value as the mass ratio increases between 0 to 1.0, while further increase of the mass ratio maintain constant maximum value. The amplitude reduction ratio against the foundation stiffness is depicted by Figure 11, where increasing the values of foundation stiffness produces a sharp decrease in the ARR between the range of 0 and 50kN/m, after which further increase produces gentle decrease in the ARR. The logarithmic damping decrement against the flow velocity and time are illustrated by Figures 12 and 13, from which the saw-tooth profiles exhibit oscillatory characteristics for various values of fluid-pipe mass ratio.

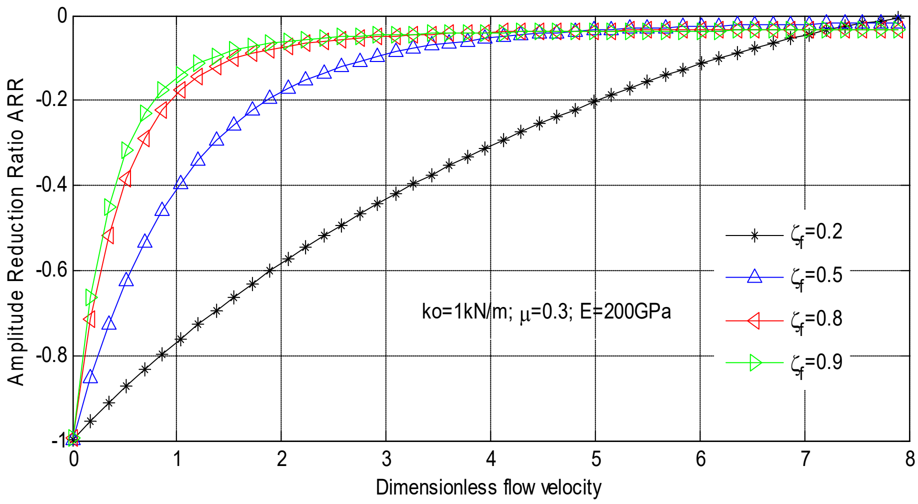

Fig. 6. Graph of $ARR = -\exp\left(-\frac{\pi\Omega_{cd}}{\sqrt{\left(\Omega_n^2 + \Omega_{cd}^2\right)}}\right)$ versus $\bar{U}$

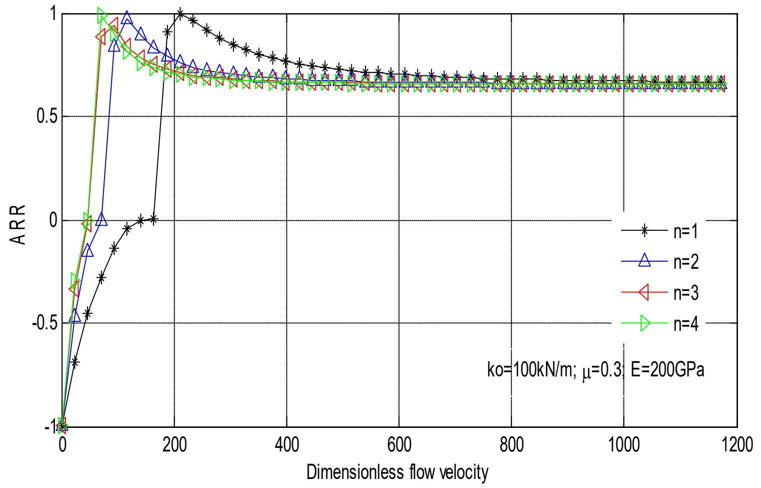

Fig. 7. Graph of $ARR = -\exp(-\frac{\pi\Omega_{cd}}{\sqrt{(\Omega_n^2 + \Omega_{cd}^2)}})$ versus $\bar{U}$

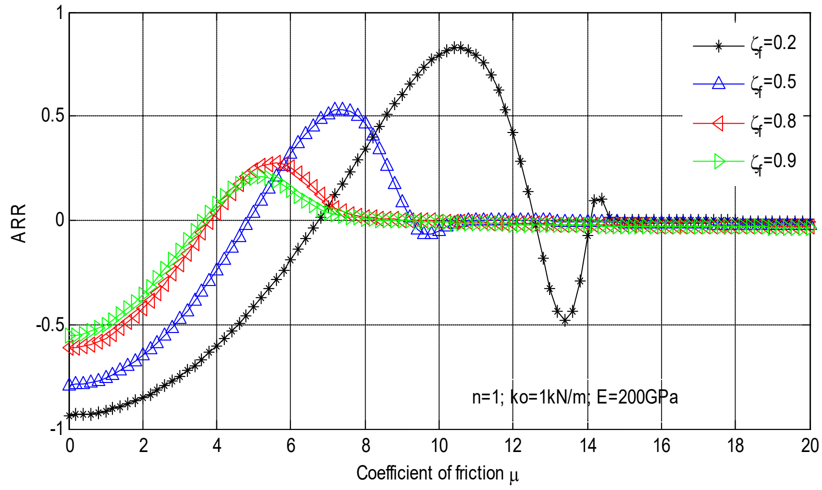

Fig. 8. Graph of $ARR = -\exp(-\frac{\pi\Omega_{cd}}{\sqrt{(\Omega_n^2 + \Omega_{cd}^2)}})$ versus μ for $U = 15m/s$

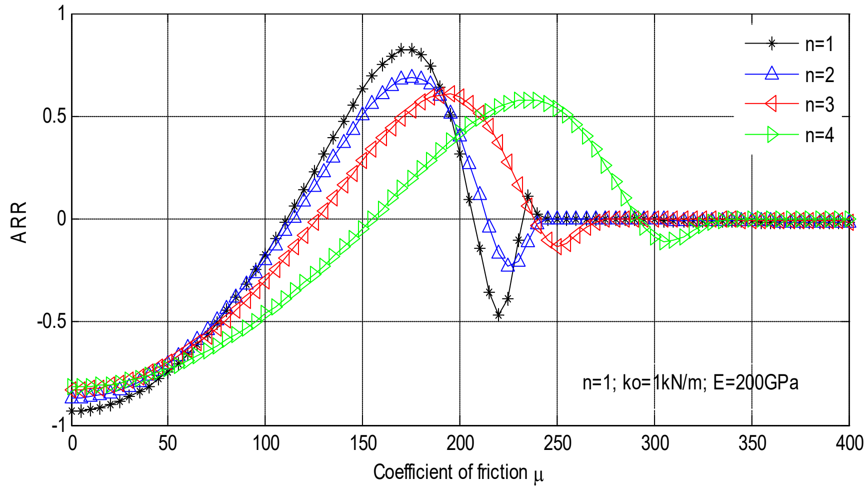

Fig. 9. Graph of $ARR = -\exp(-\frac{\pi\Omega_{cd}}{\sqrt{(\Omega_n^2 + \Omega_{cd}^2)}})$ versus μ for $U = 15m/s$

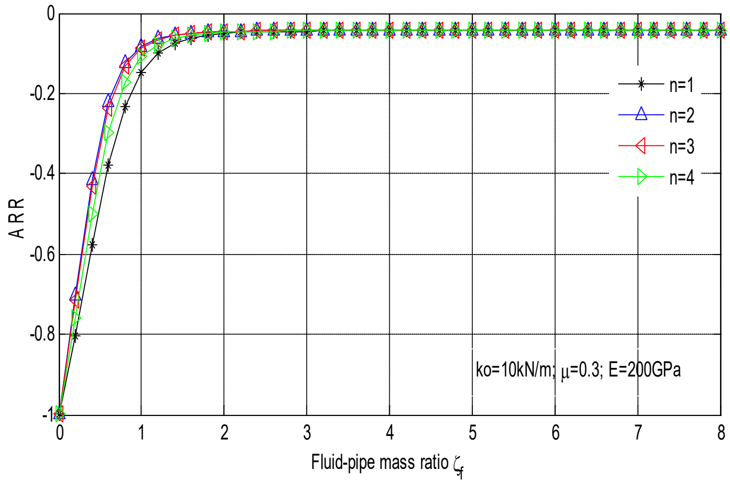

Fig. 10. Graph of $ARR = -\exp(-\frac{\pi\Omega_{cd}}{\sqrt{(\Omega_n^2 + \Omega_{cd}^2)}})$ versus ζ_f for $U = 15m/s$

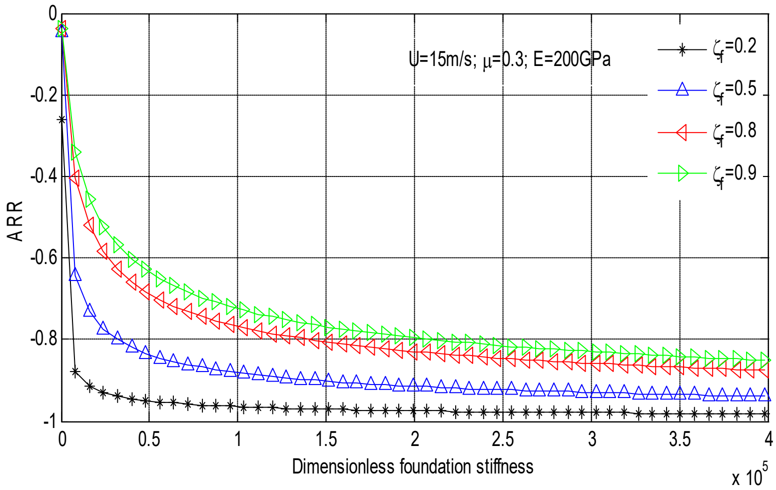

Fig. 11. Graph of $ARR = -\exp(-\frac{\pi\Omega_{cd}}{\sqrt{(\Omega_n^2 + \Omega_{cd}^2)}})$ versus $\bar{k}_0$ μ for $U = 15m/s$

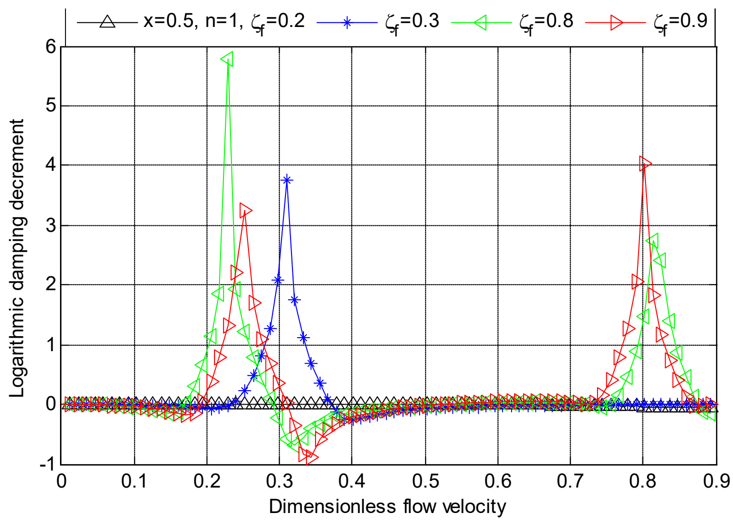

Fig. 12. Graph of $\Lambda = \frac{1}{2}\ln\left(1 + \frac{\Psi^2\Omega_{cd}}{383.2 + 3EI + \Omega_n^2}\right)$ versus $\bar{U}$

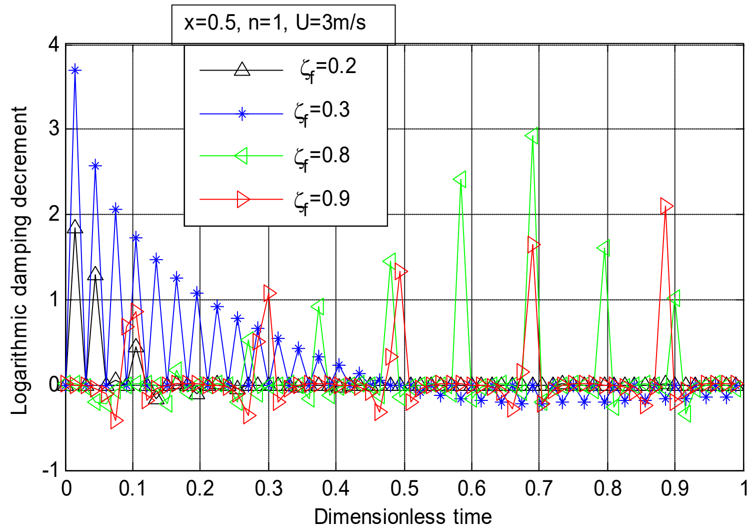

Fig. 13. Graph of $\Lambda = \frac{1}{2}\ln\left(1+\frac{\Psi^2\Omega_{cd}}{383.2+3EI+\Omega_n^2}\right)$ versus $\bar{t}$

Figures 14-17 show the bifurcation profile for the pre- and post-divergence characteristics of the pipeline system. It is shown that as the foundation stiffness increases the critical flow velocity increases (Figures 14 and 15), while increasing the fluid-pipe mass ratio decreases the critical flow velocity (Figures 16 and 17). The natural frequency of the system is demonstrated in Figures 18 through 21 where the two regions describing the divergence situation, that is, when the flow is less- and greater- than the critical flow points are shown.

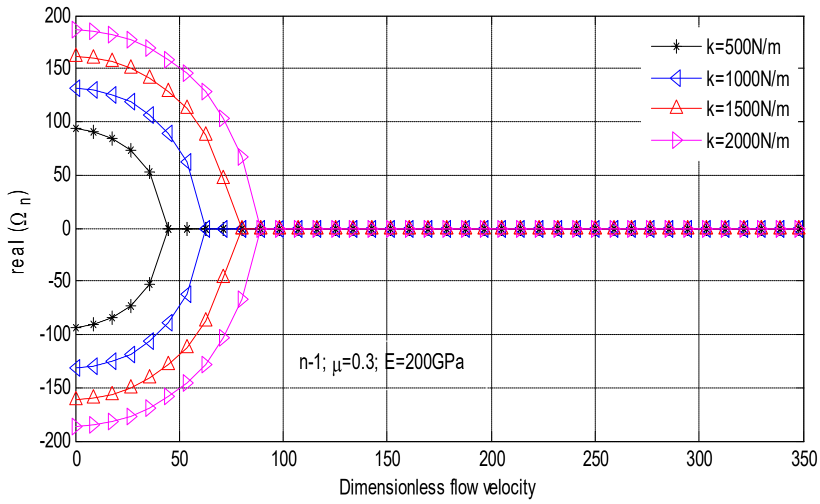

Fig. 14. Pre-divergence bifurcation profile for various values of foundation stiffnesss

It is noteworthy that the critical flow velocity increases with decreasing fluid-pipe mass ratio but with increasing modal values. Then, in Figures 22 and 23, the system's dynamic responses against the pipe length for uniform fluid flow velocity $\bar{U} = 5m/s$ are presented as exhibiting a convex or concave parabolic curvature depending on the values of mode and time. The table below gives the values of the parameters used for developing the explained figures.

Table 1. Values of Coding Parameters

Description of parameters	Values
Pipe length	30m
External radius	203mm
Internal radius	193mm
Density of pipe material	781kg/m3

Density of fluid	850 kg/m3
Elastic constant of pipe material	200x109Pa
Coefficient of friction	0.3Ns/m for of the some curves
Foundation stiffness constant	1KN/m

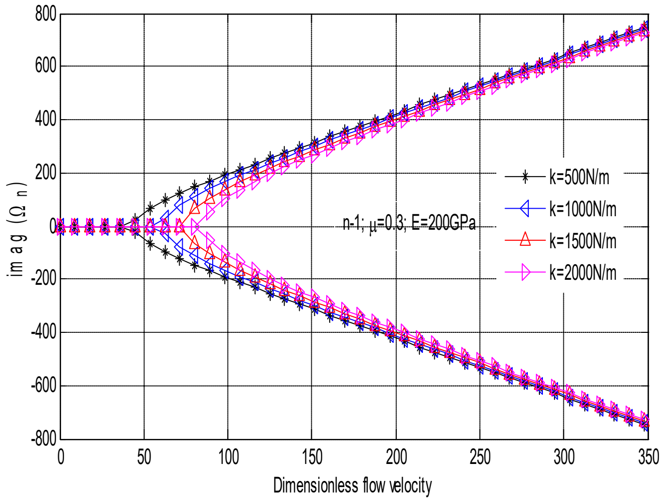

Fig. 15. Post-divergence bifurcation profile for various values of foundation stiffnesss

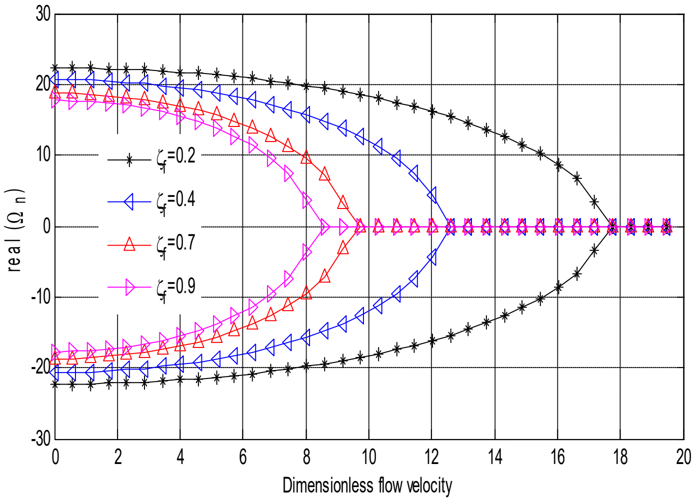

Fig. 16. Pre-divergence bifurcation profile for various values of fluid-pipe mass ratio

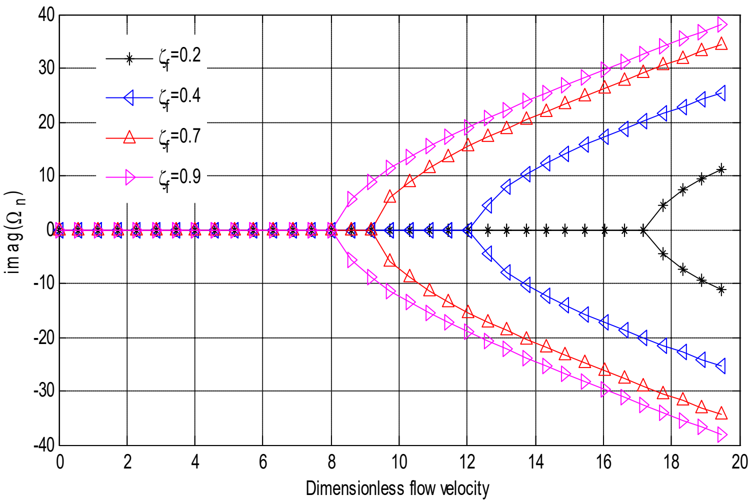

Fig. 17. Post-divergence bifurcation profile for various values of fluid-pipe mass ratio

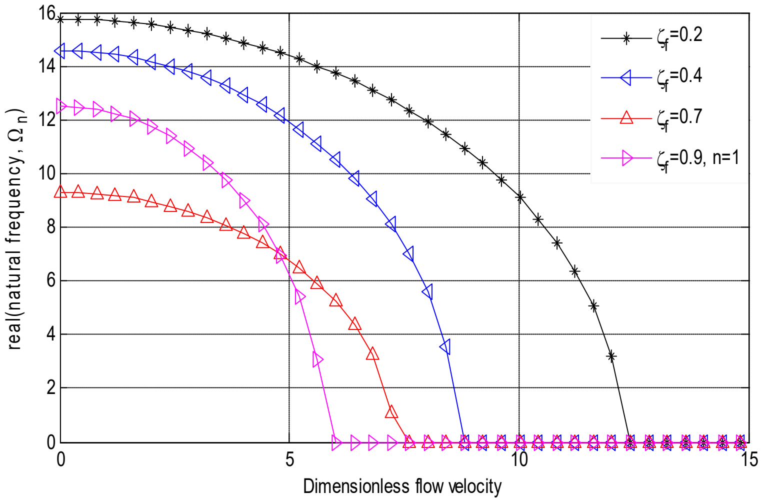

Fig. 18. Graph of *real part of* $(\Omega_n)\ \forall \bar{U} < \bar{U}_{cr}$

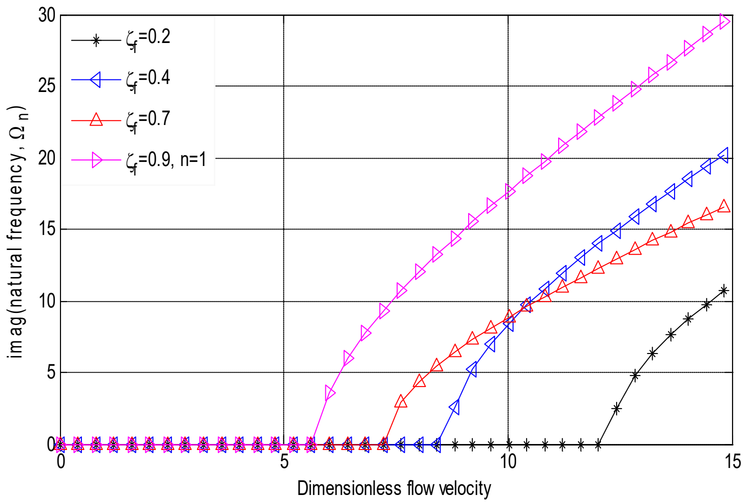

Fig. 19. Graph of *imaginary part of* $(\Omega_n)\ \forall \bar{U} > \bar{U}_{cr}$

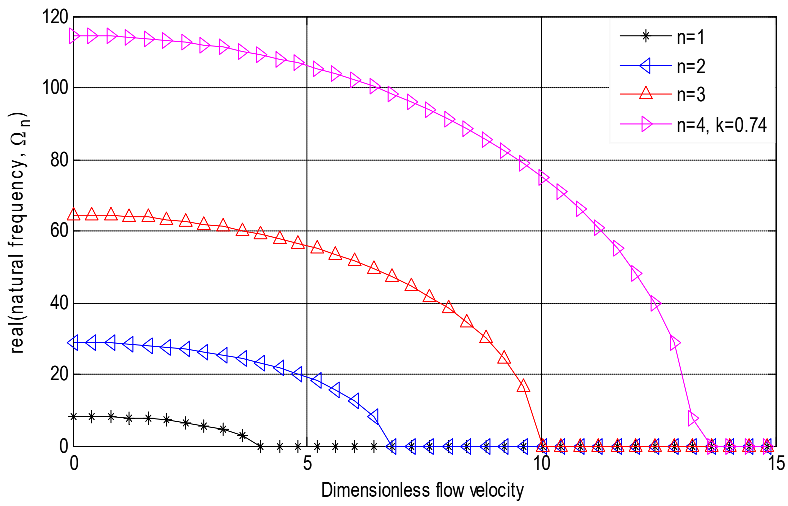

Fig. 20. Graph of *real part of* $(\Omega_n)\ \forall \bar{U} < \bar{U}_{cr}$

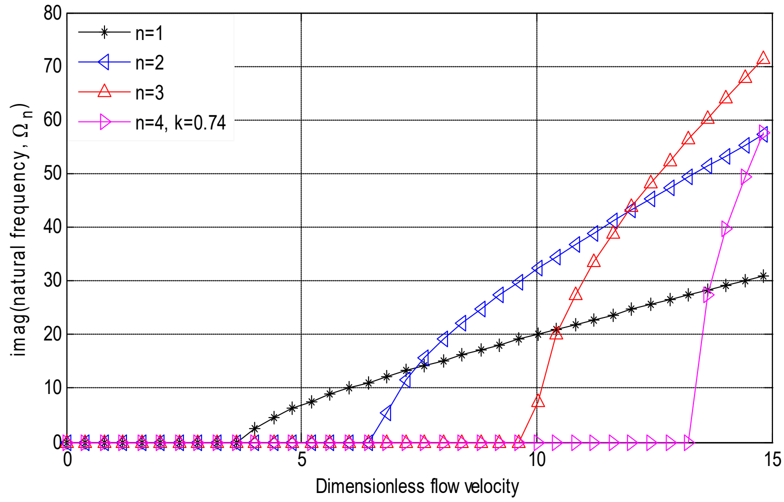

Fig. 21. Graph of $imaginary\ \ part\ \ of\ \ (\Omega_n)\ \forall\bar{U}>\bar{U}_{cr}$

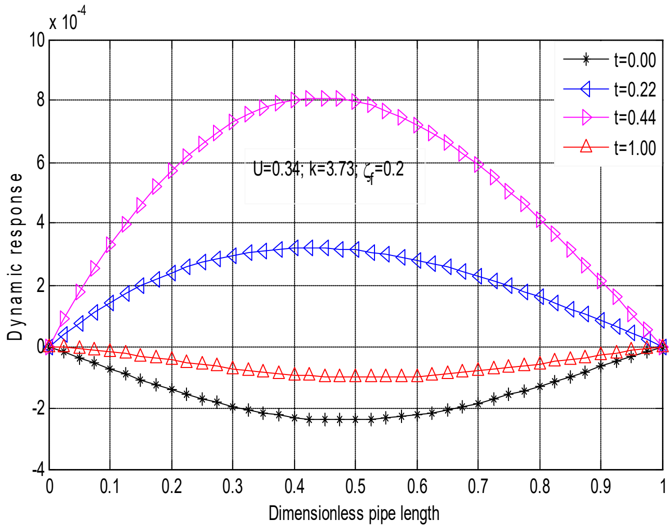

Fig. 22. Graph of dynamic response against pipe length

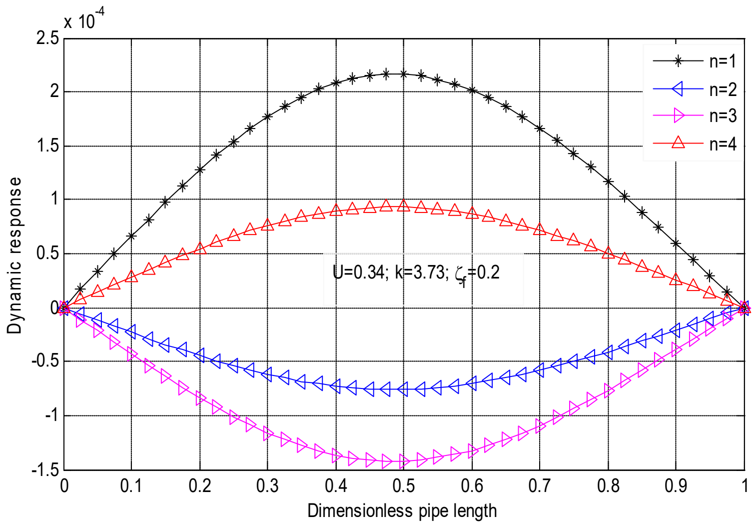

Fig. 23. Graph of dynamic response against pipe length

5. Conclusion

This paper proposes a concise analytic solution technique. The complex Fourier exponential transform in conjunction with the employment of the contrived bending moment polynomial function for the case of the pipe segment with an entrained fluid to transform the homogeneous partial differential equation of the mathematical Physics problem to an inhomogeneous ordinary differential equation in Fourier-time domain demonstrated an apt mathematical solution method that can equally be exploited for the solution of non-linear problems in conjunction with homotopy perturbation method (HPM), homotopy analysis method (HAM) and differential transformation method (DTM). It is also noteworthy to state clearly that unlike the modal complex frequencies the rationalized natural frequencies are independent of the damping and Coriolis effects, but under the modulation of flow velocities and the foundation stiffness. Results in literature are confirmed and validated in appropriate asymptotic limits. See [2], [17] and [19]. Our findings include:

1. The fluid-pipe mass ratio strongly affected both the natural frequency and the dynamic responses of the system;
2. The system's frequencies and responses are functions of the foundation stiffness k_0 and the coefficients of friction μ ;
3. For $\mu = 0.3Ns/m$, the optimum foundation is likely between 500kN/m and 1.0MN/m, while for $k = 500kN/m$, the appropriate values of $\bar{\mu}$ may be 5.0 for $\zeta_f = 0.9$ and 11.0 for $\zeta_f = 0.2$.

Nomenclature

E	Young's modulus $\left(N/m^2\right)$
I	moment of inertia $\left(m^4\right)$
ρ_s	mass density of pipe per unit length $\left(Kg/m\right)$
ρ_f	mass density of fluid per unit length $\left(Kg/m\right)$
U	internal flow velocity $\left(m/s\right)$
w	transverse deflection $\left(m\right)$
$\bar{W}$	dimensionless dynamic response
$\bar{W}_{\bar{x}}$	pipe's end slope
$\bar{W}_{\bar{x}\bar{x}}$	pipe's end moment
$\bar{W}_{\bar{x}\bar{x}\bar{x}}$	pipe's end shear force
$\bar{t}$	dimensionless time
$\bar{x}$	coordinate of pipe's neutral axis
g	gravitational acceleration $\left(m/s^2\right)$
L	pipe length $\left(m\right)$
λ	wave number
δ	damping decrement
Λ	logarithmic damping decrement
ARR	Amplitude Reduction Ratio
ς_f	fluid-pipe mass ratio
k_0	foundation stiffness N/m
$\bar{\mu}$	dimensionless coefficient of friction
Ω_0	system frequency at zero flow velocity
Ω_n	natural frequency (dimensionless)
Ω_1	complex frequency (dimensionless)
Ω_2	conjugate complex frequency (dimensionless)
Ω_{cor}	frequency due to Coriolis force (dimensionless)
Ω_{cd}	frequency due to Coriolis and damping forces (dimensionless)
$\bar{U}_{cr}$	critical flow velocity (dimensionless)

References

[1] Paidoussis, M.P. (2013) Fluid-structure interactions: slender structures and axial flows, Vol. 1, Academic Press, *Revised Edition*.
[2] Mostafa N.H. (2014) "Effect of a Viscoelastic foundation on the Dynamic Stability of a Fluid Conveying Pipe". International Journal of Applied Science and Engineering 12, 1:59-74.
[3] Paidoussis, M.P. &Issid, N.T. (1974) Dynamic stability of pipes conveying fluid. Journal of Sound and Vibration 33, 267-294.
[4] Murai, M. and Yamamoto, M. (2010) An Experimental Analysis of the Internal Flow Effects on Marine Risers. Proceedings of MARTEC 2010, P.159-165.
[5] Marakala N, Appukutttan K.K, and Kadoli R. (2014) Experimental and Theoretical Investigation of Combined Effects of Fluid and Thermal Induced Vibration on Vertical Thin Slender Tube. IOSR- JMCE, ISSN: 2278-1684, pp: 63-68.
[6] Ziegler, H. (1968) Principles of Structural Stability. Waltham, MA: Blaisdell.
[7] Lottati, I. and Kornecki, A. (1986) The effect of an elastic foundation and of dissipative forces on the stability of fluid conveying pipes. Journal of Sound and Vibration, 109(2): 327-338.
[8] Stein, R.A., Tobriner, M.W. (1970) Vibration of pipes containing flowing fluids. Trans ASME J Appl. Mechanics; 906-916.
[9] Dermendjian-Ivanova, D.S. (1992) Critical flow velocities of a simply supported pipeline on an elastic foundation. J Sound Vibration; 157: 370-374.
[10] Chary, S.R., Rao, C.K., Iyengar, R.N. (1993) Vibration of Fluid Conveying Pipe on Winkler Foundation, Proceedings of the 8th National Convention of Aerospace Engineers on Aeroelasticity, Hydroelasticity and other Fluid-Structure Interaction Problems, IIT Kharagpur, India; pp. 266-287.
[11] Doaré, O., de Langre, O. (2002) Local and global instability of fluid conveying pipes on elastic foundation. J Fluids &Structures; 16: 1-14.
[12] Chellapilla, K.R. and Simha, H.S. (2008) Vibrations of Fluid-Conveying Pipes Resting on Two-Parameter Foundation. The Open Acoustics Journal, 1, 24-33.
[13] Mahrenholtz, O. H. (2010) Beam on viscoelastic foundation: an extension of Winkler's model. Archive of Applied Mechanics, 80(1): 93-102.
[14] Saxena, A. and Patel, R.K. (2013) Vibration Control of Cantilever Beam Using Eddy Current Damper. International Journal of Engineering and Innovative Technology (IJESIT) Volume 2, Issue 3.

[15] Jae-ung, B., Moon, K.K. and Daniel, J.I. (2005) Vibration Suppression of a Cantilever Beam Using Eddy Current Damper. Journal of Sound and Vibration 284, 805-824.
[16] Tonoli, A. (2007) Dynamic characteristics of Eddy current dampers and couplers. Journal of Sound and Vibration 301: 576-591.
[17] Olayiwola, P.S. (2016) Mechanics of a Fluid-Conveying Pipeline System Resting on a Viscoelastic Foundation. Journal of Multidisciplinary Engineering Science Studies (JMESS), ISSN: 2458-925X Vol. 2. Issue 3.
[18] Szmidt T and Przybylowicz P. (2013) Critical Flow Velocity with Electromagnetic Actuators. Journal of Theoretical and Applied Mechanics 51, 2, pp. 487-496.
[19] Kuye, S.I. (2013) Analysis of the Dynamics of Offshore Fluid-Conveying Viscoelastic Pipes Resting on a Deformable Sea Bed. Journal of Emerging Trends in Engineering and Applied Sciences (JETEAS) 4(5): 742-751.
[20] Jeffrey A. (2002) Advanced Engineering Mathematics, Harcourt Academic Press. U.S.A, p.596.
[21] Wrede, R. C. and Spiegel, M. (2002) Thoery and Problems of Advanced Calculus 2nd Ed. Schaum's Outline Serises, McGraw-Hill, p. 364.
[22] Nash, W. A. (1977) Thoery and Problems of Strength of Materials, 2nd Ed. Schaum's Outline Series, McGraw-Hill, p. 83, 159-161.
[23] Cole E.B. (1960) Theory of Vibrations. The University of Liverpool.
[24] Darkov, A. (1983) Structural Mechanics. Mir Publishers, Moscow.